

# Exploring the Properties and Optical Sensing Capability of Sol–Gel Materials Containing a Covalently Bonded Binucleating Cryptand

Manuel G. Basallote,<sup>\*,†</sup> Eduardo Blanco,<sup>‡</sup> Miguel Blázquez,<sup>‡</sup>  
María J. Fernández-Trujillo,<sup>†</sup> Rocío Litrán,<sup>‡</sup> M. Angeles Máñez,<sup>†</sup> and  
Milagrosa Ramírez del Solar<sup>‡</sup>

*Departamento de Ciencia de los Materiales e Ingeniería Metalúrgica y Química Inorgánica  
and Departamento de Física de la Materia Condensada, Universidad de Cádiz,  
Facultad de Ciencias, Apartado 40, 11510-Puerto Real (Cádiz), Spain*

*Received October 22, 2002. Revised Manuscript Received February 10, 2003*

A large octaaza cryptand containing two tris(2-aminoethyl)amine (*tren*) donor subunits and six  $-\text{Si}(\text{OEt})_3$  pendant groups has been synthesized and used to prepare monolithic samples of sol–gel materials containing the cryptand covalently bonded to the silica network. Despite the constraints imposed by the multiple bonds to the network, the cryptand maintains its ability to form a binuclear Cu(II) complex and to interact with an ancillary azide ligand. A large number of reaction cycles involving the formation of the Cu(II) complex, the interaction with azide, and decomposition by treatment with an excess of acid can be carried out and easily monitored through the spectral changes in the Vis region. Adsorption studies indicate a mesoporous nature for these materials, with the pore size increasing with the cryptand content. The formation of the Cu(II) complex causes a significant decrease in the intensity of the  $\text{Q}_3$  band in the  $^{29}\text{Si}$  NMR spectra, which suggests that the cryptand is placed preferentially in  $\text{Q}_3$ -rich sites. The capability of these materials for optical sensing of the azide anion has been explored. Although the absorbance changes show a linear dependence with the azide concentration up to  $1 \times 10^{-3}$  M, kinetic studies indicate a long response time caused by slow diffusion of the reagents through the cavity network of the monoliths.

## Introduction

The preparation of inorganic–organic hybrid materials by sol–gel procedures is a topic of current interest, and several reviews have been published in recent years covering different aspects of the chemistry of these materials.<sup>1–8</sup> From the point of view of optical sensing, one of the advantages of sol–gel materials is the possibility of using a large variety of molecules or ions as receptors, which facilitates selective sensing.<sup>9–17</sup> Moreover, covalent bonding of the receptor to the silica

network<sup>18–23</sup> avoids the leaching problems associated with materials with physically trapped receptors and leads to solids with more reproducible properties. Although the development of useful sensors based on sol–gel materials can be conditioned by long-term changes in the properties of these materials and by the slow diffusion of the species through their cavity networks, significant advances have been achieved in the last few years and several useful sensors have been reported.<sup>24–29</sup> Thus, it has been shown that the adequate choice of

\* To whom correspondence should be addressed. Phone: +34 956 016398. Fax: +34 956 016288. E-mail: manuel.basallote@uca.es.

<sup>†</sup> Departamento de Ciencia de los Materiales e Ingeniería Metalúrgica y Química Inorgánica.

<sup>‡</sup> Departamento de Física de la Materia Condensada.

(1) MacKenzie, J. D.; Bescher, E. P. *J. Sol-Gel Sci. Technol.* **1998**, *13*, 371.

(2) Collinson, M. M. *Crit. Rev. Anal. Chem.* **1999**, *29*, 289.

(3) Corriu, R. J. P. *Angew. Chem., Int. Ed.* **2000**, *39*, 1376.

(4) Shea, K. J.; Loy, D. A. *Chem. Mater.* **2001**, *13*, 3306.

(5) Keeling-Tucker, T.; Brennan, J. D. *Chem. Mater.* **2001**, *13*, 3331.

(6) Walcarius, A. *Chem. Mater.* **2001**, *13*, 3351.

(7) Scott, B. J.; Wirnsberger, G.; Stucky, G. D. *Chem. Mater.* **2001**, *13*, 3140.

(8) Schulz-Ekloff, G.; Wöhrle, D.; Van Duffel, B.; Schoonheydt, R. A. *Microporous Mesoporous Mater.* **2002**, *51*, 91.

(9) Fu, L.; Zhang, H.; Wang, S.; Meng, Q.; Yang, K.; Ni, J. *J. Sol-Gel Sci. Technol.* **1999**, *15*, 49.

(10) McCraith, B. D.; McDonagh, C.; McEvoy, A. K.; Butler, T.; O'Keeffe, G.; Murphy, V. J. *Sol-Gel Sci. Technol.* **1997**, *8*, 1053.

(11) Bendavid, O.; Shafir, E.; Gilath, I.; Prior, Y.; Avnir, D. *Chem. Mater.* **1997**, *9*, 2255.

(12) Murtagh, M. T.; Shahriari, M. R.; Krihak, M. *Chem. Mater.* **1998**, *10*, 3862.

(13) Hartnett, A. M.; Ingersoll, C. M.; Baker, G. A.; Bright, F. V. *Anal. Chem.* **1999**, *71*, 1215.

(14) Leventis, N.; Elder, I. A.; Rolison, D. R.; Anderson, M. L.; Merzbacher, C. I. *Chem. Mater.* **1999**, *11*, 2837.

(15) Pandey, S.; Baker, G. A.; Kane, M. A.; Bonzagni, N. J.; Bright, F. V. *Chem. Mater.* **2000**, *12*, 3547.

(16) McCraith, B. D.; McDonagh, C. M.; O'Keeffe, G.; McEvoy, A. K.; Butler, T.; Sheridan, F. R. *Sens. Actuators, B* **1995**, *29*, 51.

(17) Bescher, E.; Mackenzie, J. D. *Mater. Sci. Eng., C* **1998**, *6*, 145.

(18) Kloster, G. M.; Taylor, C. M.; Watton, S. P. *Inorg. Chem.* **1999**, *38*, 3954.

(19) Dubois, G.; Corriu, R. J. P.; Reyé, C.; Brandès, S.; Denat, F.; Guillard, R. *Chem. Commun.* **1999**, 2283.

(20) Tien, P.; Chau, L. K. *Chem. Mater.* **1999**, *11*, 2141.

(21) Lobnik, A.; Oehme, I.; Murkovic, I.; Wolfbeis, O. *Anal. Chim. Acta* **1998**, *367*, 159.

(22) Chuit, C.; Corriu, R. J. P.; Dubois, G.; Reyé, C. *Chem. Commun.* **1999**, 723.

(23) McEvoy, A. K.; McDonagh, C.; McCraith, B. D. *Analyst* **1996**, *121*, 785.

(24) Villegas, M. A.; Pascual, L. *Thin Solid Films* **1999**, *351*, 103.

(25) McDonagh, C.; Bowe, P.; Mongey, K.; McCraith, B. D. *J. Non-Cryst. Solids* **2002**, *306*, 138.

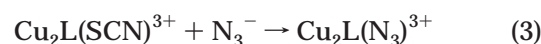
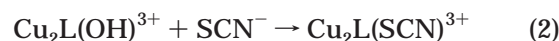
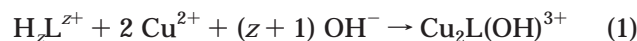
(26) Cajlakovic, M.; Lobnik, A.; Werner, T. *Anal. Chim. Acta* **2002**, *455*, 207.

starting materials and preparation conditions allows the preparation of sensors with a rapid response and stability for weeks or months.<sup>30–32</sup> In addition, some procedures have been also developed recently to reduce the response time and to increase the long-term stability of these kinds of sensors.<sup>33–35</sup>

On the other hand, the development of sensors for the determination of anions is also a field of current interest, mainly because of its biological and environmental relevance.<sup>36</sup> In particular, the azide anion is a respiratory poison and there is considerable interest in analytical methods for its determination.<sup>37–40</sup> The ability of using large polyaza macrocycles and cryptands, and their metal complexes, for the selective recognition of anions is well-known.<sup>41–47</sup> The existence of several nitrogen donors in this kind of ligand makes possible the formation of highly protonated  $H_zL^{z+}$  species that bind anions through electrostatic interaction with the protonated amine groups. Metal complexes of these ligands also contain additional coordination sites that can be used for binding anions as ancillary ligands. For the case of cryptand L, the cavity is large enough to accommodate two metal ions, which leads to the formation of stable binuclear metal complexes with one metal ion coordinated to each one of the tris(2-aminoethyl)-amine (*tren*) donor subunits.<sup>48–50</sup> These binuclear Cu(II)–L complexes have been shown to form stable  $Cu_2LX^{z+}$  complexes with several X ligands, with the stability of these species depending on the charge and steric characteristics of the X ancillary ligand.<sup>47</sup> Thus,

for singly charged  $X^-$  ligands there is a maximum stability for  $N_3^-$ , which has been interpreted in terms of a better fit between the cavity size and the bite length of the anion.

In a previous paper<sup>51</sup> we have shown that L can be trapped into a sol–gel matrix maintaining its ability to react reversibly with  $Cu^{2+}$ ,  $SCN^-$ ,  $N_3^-$ , and  $H^+$ , thus allowing reaction cycles of the type shown in eqs 1–4.



Whereas  $Cu^{2+}$ ,  $SCN^-$ , and  $N_3^-$  are readily exchanged with an external solution, the larger size of the  $H_zL^{z+}$  species hinders its mobility through the cavity network of the sol–gel material and keeps the cryptand trapped. The different absorption spectra of the complexes involved in eqs 1–4 allows easy monitoring of the reaction cycles and makes these materials good candidates for anion sensing. However, the release of a significant fraction of the L cryptand in each reaction cycle leads to a lack of reproducibility that prevents the use of these materials under practical conditions.

In the present paper we report the synthesis of the related L' cryptand, which contains six hydrolyzable *n*-propyltriethoxysilane groups to be used for a covalent binding to the sol–gel network. Xerogel materials prepared from L' show a chemical behavior similar to those prepared from L but they do not release the cryptand, which has allowed us to carry out additional studies on the interaction with  $Cu^{2+}$  and the azide anion.

(27) Calvo-Muñoz, M. L.; Truong, T. T.; Tran-Thi, T. H. *Sens. Actuators, B* **2002**, *87*, 173.

(28) Li, C. I.; Lin, Y. H.; Shih, C. L.; Tsauro, J. P.; Chau, L. K. *Biosens. Bioelectron.* **2002**, *17*, 323.

(29) Chen, X.; Hu, Y.; Wilson, G. S. *Biosens. Bioelectron.* **2002**, *17*, 1005.

(30) Von Bültzingslöwen, C.; McEvoy, A. K.; McDonald, C.; Mac-Craith, B. D.; Klimant, I.; Krause, C.; Wolfbeis, O. S. *Analyst* **2002**, *127*, 1478.

(31) Nivens, D. A.; Schiza, M. V.; Angel, S. M. *Talanta* **2002**, *58*, 543.

(32) Dubois, G.; Reyé, C.; Corriu, R. J. P.; Brandès, S.; Denat, F.; Guillard, R. *Angew. Chem., Int. Ed.* **2001**, *40*, 1087.

(33) Chen, X.; Zhong, Z.; Li, Z.; Jiang, Y.; Wang, X.; Wong, K. *Sens. Actuators, B* **2002**, *87*, 233.

(34) Ismail, F.; Malins, C.; Goddard, N. J. *Analyst* **2002**, *127*, 253.

(35) Rayss, J.; Sudolski, G. *Sens. Actuators, B* **2002**, *87*, 397.

(36) Amendola, V.; Fabbri, L.; Mangano, C.; Pallavicini, P.; Poggi, A.; Taglietti, A. *Coord. Chem. Rev.* **2001**, *219–221*, 821.

(37) Gennaro, M. C.; Abrigo, C.; Marengo, E.; Liberatori, A. J. *Liquid Chromatogr.* **1993**, *16*, 2715.

(38) Hassan, S. S. M.; Ahmed, M. A.; Marzouk, S.; Elnemma, E. M. *Anal. Chem.* **1991**, *63*, 1547.

(39) Daigle, F.; Trudeau, F.; Robinson, G.; Smyth, M. R.; Leech, D. *Biosens. Bioelectron.* **1998**, *13*, 417.

(40) Leech, D.; Daigle, F. *Analyst* **1998**, *123*, 1971.

(41) Morgan, G.; McKee, V.; Nelson, J. *J. Chem. Soc., Chem. Commun.* **1995**, 1649.

(42) Fabbri, L.; Francese, G.; Licchelli, Perotti, A.; Taglietti, A. *Chem. Commun.* **1997**, 581.

(43) Fabbri, L.; Faravelli, I.; Francese, G.; Licchelli, M.; Perotti, A.; Taglietti, A. *Chem. Commun.* **1998**, 971.

(44) Mason, S.; Clifford, T.; Seib, L.; Kuczera, K.; Bowman-James, K. *J. Am. Chem. Soc.* **1998**, *120*, 8899.

(45) Hynes, M. J.; Maubert, B.; McKee, V.; Town, R. M.; Nelson, J. *J. Chem. Soc., Dalton Trans.* **2000**, 2853.

(46) Maubert, B. M.; Nelson, J.; McKee, V.; Town, R. M.; Pál, I. J. *Chem. Soc., Dalton Trans.* **2001**, 1395.

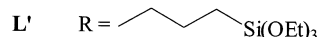
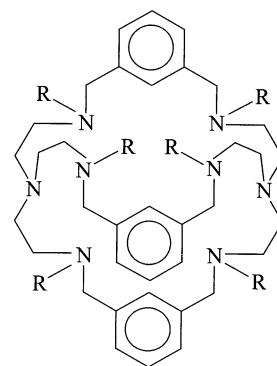
(47) Fabbri, L.; Pallavicini, P.; Parodi, L.; Taglietti, A. *Inorg. Chim. Acta* **1995**, *238*, 5.

(48) Menif, R.; Reibenspies, J.; Martell, A. E. *Inorg. Chem.* **1991**, *30*, 3446.

(49) Basallote, M. G.; Durán, J.; Fernández-Trujillo, M. J.; Máñez, M. A. *J. Chem. Soc., Dalton Trans.* **2002**, 2074.

(50) Basallote, M. G.; Durán, J.; Fernández-Trujillo, M. J.; Máñez, M. A. *J. Chem. Soc., Dalton Trans.* **1999**, 3817.

Scheme 1



## Results and Discussion

**Sample Preparation.** The silylated cryptand L' was prepared from reaction of L with  $Cl(CH_2)_3Si(OEt)_3$  following the procedure described in the Experimental

(51) Basallote, M. G.; Blanco, E.; Fernández-Trujillo, M. J.; Máñez, M. A.; Ramírez del Solar, M. *Chem. Mater.* **2002**, *14*, 670.

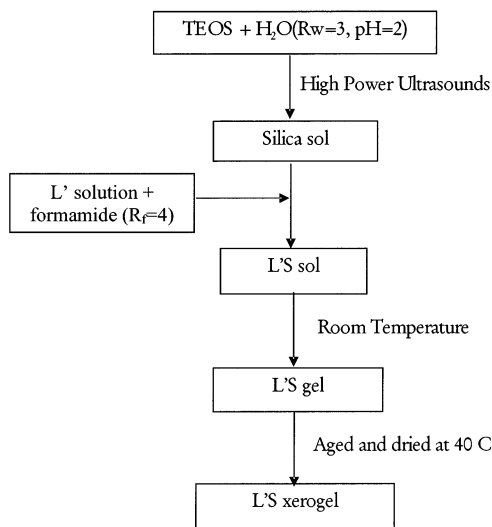


**Figure 1.** Schematic representation of the sol–gel processing steps for preparation of the L'-containing sonogel samples.

Section. It was isolated as an oily liquid and characterized by NMR spectroscopy. From the first preparations, L' revealed to be difficult to handle because it readily hydrolyzes to give a complex mixture of products, and so, we decided to prepare and store the cryptand under an inert atmosphere of argon. In this way, solutions of L' in CD<sub>3</sub>CN yielded reproducible <sup>1</sup>H, <sup>13</sup>C{<sup>1</sup>H}, and <sup>29</sup>-Si{<sup>1</sup>H} NMR spectra that confirm the nature and purity of the product, although the spectra recorded several days after the NMR samples were prepared showed clear evidence of hydrolysis by reaction with traces of water, which prevents storage of L' for long times. To avoid problems associated with hydrolysis of the cryptand, monoliths of L'-containing sol–gel materials were prepared from solutions of freshly prepared (less than 1 day) cryptand samples.

A schematic presentation of the procedure for preparation of the xerogels is shown in Figure 1 and the details are given in the Experimental Section. After ultrasound-promoted prehydrolysis of TEOS, different amounts of an L' (or L) solution were added to obtain homogeneous hybrid sols that gel after 1–4 days at room temperature. In some cases, CuSO<sub>4</sub> was added to the hydrolysis water to achieve the formation of the Cu–L' complex before gelification. The xerogels obtained after drying are labeled in the paper as *nL'S*, *nLS*, and *nL'CuS*, where L or L' indicates the cryptand used, S refers to sonogel, and *n* is a measure of the relative content of cryptand in the sample, expressed as  $n = 10^5 [L']/[TEOS]$ , where the concentrations ratio is that achieved after addition of the cryptand to the silica sol. When a Cu<sup>2+</sup> salt is added, the symbol Cu is also included in the sample code. All the xerogels were obtained as monolithic pieces whose approximate dimensions were 15 × 5 × 5 mm.

**Reactivity of the Sol–Gel Materials Toward Cu<sup>2+</sup>, N<sub>3</sub><sup>-</sup>, and H<sup>+</sup>.** The reactivity behavior of the unsubstituted L cryptand toward Cu(II), acid, and ancillary ligands as SCN<sup>-</sup> or N<sub>3</sub><sup>-</sup>, has been described in previous works.<sup>49,51</sup> The L cryptand reacts with Cu<sup>2+</sup> both in aqueous solution and trapped into sol–gel matrixes, the reaction product in the presence of an excess of the metal ion being the binuclear Cu<sub>2</sub>L(OH)<sup>3+</sup> complex (eq 1). Addition of an excess of an ancillary

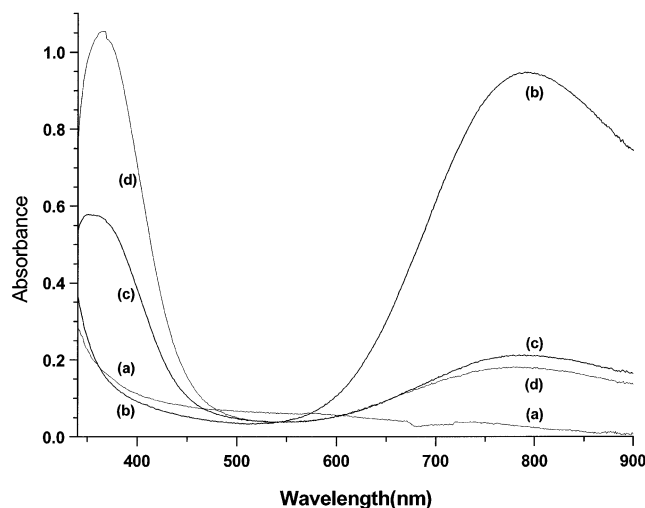


**Figure 2.** Visible absorption spectra of the 5L'Cu sample at different stages of a reaction cycle: (a) sample washed with water, (b) after treatment with 0.10 M CuSO<sub>4</sub> solution, (c) after treatment with a 1 × 10<sup>-3</sup> M azide solution, and (d) after treatment with a 2.5 × 10<sup>-3</sup> M azide solution. In all cases the sample was washed with water during 1–2 h before recording the spectrum.

ligand such as thiocyanate or azide leads to substitution of the coordinated OH<sup>-</sup> ligand to form Cu<sub>2</sub>LX<sup>3+</sup> (X<sup>-</sup> = SCN<sup>-</sup>, N<sub>3</sub><sup>-</sup>; eqs 2 and 3). All the binuclear complexes decompose in the presence of an excess of acid to yield Cu<sup>2+</sup>, X<sup>-</sup>, and protonated H<sub>2</sub>L<sup>z+</sup> cryptand (eq 4, *z* = 6 when a large excess of H<sup>+</sup> is used). All these reactions can be easily monitored both in solution and in monolithic sol–gel materials by following the UV–vis absorption spectra. In the presence of Cu(II) ions, all the complexes exhibit a band centered at 800–850 nm typical of trigonal bipyramidal coordination environments about the metal ions.<sup>49,50</sup> However, the most evident changes in the absorption spectra are observed for the formation of Cu<sub>2</sub>L(N<sub>3</sub>)<sup>3+</sup>, which has a characteristic absorption band centered at 400–415 nm in aqueous solution<sup>47,49</sup> that shifts to 440 nm when trapped into sol–gel matrixes.<sup>51</sup>

Preliminary experiments with monoliths prepared from L' showed a reactivity behavior similar to that described for the related L-containing xerogels, which indicates that the covalently bonded cryptand maintains its ability to adopt the conformation required for complex formation. The major difference is that, as expected, monoliths prepared with L' lack ligand leaching and a large number of reaction cycles can be carried out. Actually, we have found that the lifetime of the monoliths is usually conditioned by its mechanical properties and not by the loss of reactivity toward external reagents. If the monolith is resistant to being broken, a large undefined number of reaction cycles as shown in eqs 1–4 can be carried out.

All the samples studied reveal a similar chemical behavior regarding the formation of the Cu(II) complex, substitution with azide, and decomposition upon addition of an excess of acid. Figure 2 shows the absorption spectra of the 5L'S sample at different stages of the reaction cycle. The initial spectrum does not show any significant absorption feature (Figure 2a). After washing with water, the L'CuS samples and the L'S samples previously treated with a 0.1 M Cu(NO<sub>3</sub>)<sub>2</sub> solution show

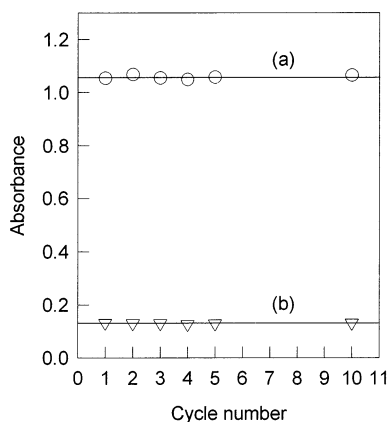


**Figure 3.** Absorbance values at 375 (a) and 800 (b) nm for the  $\text{Cu}_2\text{L}'(\text{N}_3)^{3+}$  complex in the 5L'S sample as a function of the number of cycles of reactions with  $\text{Cu}^{2+}$ ,  $\text{N}_3^-$ , and  $\text{H}^+$ .

the spectrum typical of the binuclear Cu–L' complexes (Figure 2b). Once the complex-containing sonogel is treated with a 0.001 M  $\text{NaN}_3$  solution, a color change from blue to green is observed, a behavior consistent with formation of the  $\text{Cu}_2\text{L}'(\text{N}_3)^{3+}$  complex, which indicates that the multiple covalent bonding of the cryptand to the solid network does not prevent it from adopting the conformation required to form the binuclear complex with a bridging azide. At this stage, the absorption spectra (Figure 2c and d) show the azide band (maximum at 375 nm) and a  $d-d$  band of lower intensity. No significant displacements of the absorption maximum are observed when the concentration of the Cu(II) and azide solutions is changed. Although the position of the azide band differs significantly from that observed for the related L complex trapped in sol–gel materials, it is within the range observed in solution for the azide to Cu(II) charge-transfer band.<sup>52–56</sup> After formation of the azide complex, treatment of the samples with an excess of acid leads to discoloration with disappearance of the absorption bands. A new treatment with the Cu(II) solution regenerates the Cu–L' complex and closes the reaction cycle. The reproducibility of the absorbance measurements during the reaction cycles is illustrated in Figure 3, which shows that the intensity of the bands at 375 and 800 nm for the  $\text{Cu}_2\text{L}'(\text{N}_3)^{3+}$  complex remains constant after 10 cycles of reaction with  $\text{Cu}^{2+}$ ,  $\text{N}_3^-$ , and  $\text{H}^+$ , thus confirming that covalent bonding of the cryptand avoids the leaching problems previously observed for L-containing sonogels.<sup>51</sup>

**NMR Spectra and Adsorption Isotherms of the L'-Containing Xerogels.** The molecule of the silylated L' cryptand contains 18 hydrolyzable groups, and treatment with water leads to extensive hydrolysis and polycondensation processes that will occur with a kinetics different from that of TEOS. As the samples were prepared through the joint treatment of L' and TEOS, the solid network of the resulting materials contains Si

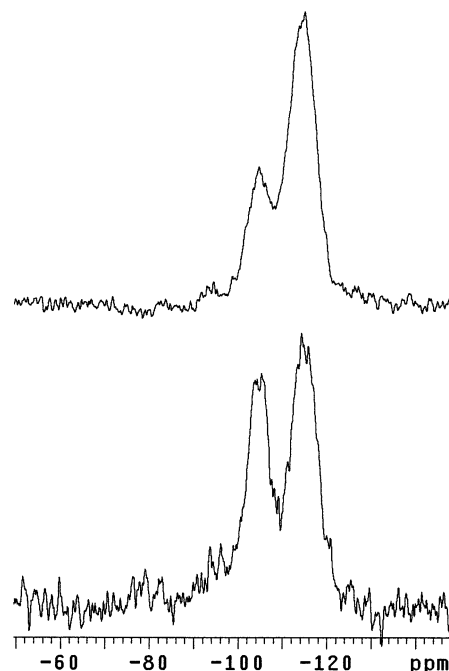


**Figure 4.**  $^{29}\text{Si}$  MAS NMR spectra of the 50L'S (bottom) and 50L'CuS (top) samples.

atoms derived from both reagents, and some information about the way in which addition of L' changes the structural properties of the TEOS-derived xerogels<sup>57</sup> was considered useful. For this reason, the  $^{29}\text{Si}$  NMR spectra and the adsorption isotherms of the samples were also studied.

The  $^{29}\text{Si}$  NMR spectra of all the xerogels prepared in this work show the same pattern: the most intense signal is always  $\text{Q}_4$  (Si atoms bonded to 4 other Si through Si–O–Si bonds), although there is also a significant  $\text{Q}_3$  signal; the  $\text{Q}_2$  signal is usually of very low intensity (Figure 4). The chemical shifts for these signals in all cases are similar to those observed for related TEOS-derived sol–gel materials.<sup>58–63</sup> Because of the low concentration of L' in the samples, the  $\text{T}_3$  signal corresponding to Si atoms of the cryptand could not be observed.

The chemical shifts of the signals do not show significant changes with the nature of the sample, but the relative intensities of the  $\text{Q}_3$  and  $\text{Q}_4$  signals ( $I_{3/4}$ ) depend on the preparation conditions (Table 1). For the reference sample B, which contains only TEOS, both signals have almost the same intensity ( $I_{3/4} = 0.92$ ). The presence of either trapped L cryptand or silylated L' cryptand covalently bonded to the TEOS-derived network only causes a small decrease of the quotient. The

(57) Blanco, E.; García-Hernández, M.; Jiménez-Riobóo, R.; Litrán, R.; Prieto, C.; Ramírez-del-Solar, M. *J. Sol-Gel Sci. Technol.* **1998**, *13*, 451.

(58) Bied, C.; Gauthier, D.; Moreau, J. J. E.; Man, M. W. C. *J. Sol-Gel Sci. Technol.* **2001**, *20*, 313.

(59) Barrera-Solano, M. C.; de la Rosa-Fox, N.; Esquivias, L. *J. Non-Cryst. Solids* **1992**, *147–148*, 194.

(60) Fidalgo, A.; Nunes, T. G.; Ilharco, L. M. *J. Sol-Gel Sci. Technol.* **2000**, *19*, 403.

(61) Abidi, N.; Deroide, B.; Zanchetta, J. V.; de Menorval, L. C.; d'Espinose, J. B. *J. Non-Cryst. Solids* **1998**, *231*, 49.

(62) Duval, E.; Bovier, C.; Roux, H.; Serughetti, J.; Tuel, A.; Wicker, G. *J. Non-Cryst. Solids* **1995**, *189*, 101.

(63) Kröcher, O.; Köppel, R. A.; Fröba, M.; Baiker, A. *J. Catal.* **1998**, *178*, 284.

(52) Goher, M. A. S.; Abu-Youssef, M. A. M.; Mautner, F. A. *Polyhedron* **1998**, *17*, 3305.

(53) Goher, M. A. S.; Al-Salem, N. A.; Mautner, F. A.; Klepp, K. O. *Polyhedron* **1997**, *16*, 825.

(54) Li, S. A.; Li, D. F.; Duan, C. Y.; Xia, J.; Yang, D. X.; Tang, W. X. *Inorg. Chem. Commun.* **2001**, *4*, 651.

(55) Goher, M. A. S.; Escuer, A.; Mautner, F. A.; Al-Salem, N. A. *Polyhedron* **2001**, *20*, 2971.

(56) Tuzcek, F.; Solomon, E. I. *Coord. Chem. Rev.* **2001**, *219–221*, 1075.

**Table 1. Relative Intensities of the Q<sub>3</sub> and Q<sub>4</sub> Bands in the <sup>29</sup>Si NMR Spectra of Xerogels**

sample	$I_{3/4}$ <sup>a</sup>
B <sup>b</sup>	0.92
800LS <sup>c</sup>	0.77
5L'S	0.53
25L'S	0.83
50L'S	0.78
500L'S	0.73
5L'/CuS	0.40
50L'/CuS	0.39
5L'S + Cu <sup>2+</sup>	0.41
25L'S + Cu <sup>2+</sup>	0.50

<sup>a</sup> Magnitude  $I_{3/4}$  represents the quotient between the intensities of both bands. <sup>b</sup> Blank silica sonogel. <sup>c</sup> Sample containing trapped L.

values of  $I_{3/4}$  for all these samples are in the 0.7–0.8 range, except for the 5L'S sample that shows an unexpectedly low value of 0.53.

The presence of Cu<sup>2+</sup> ions in the solutions used to prepare the sol–gel materials causes more important changes in the appearance of the spectra: the signal-to-noise ratio increases and the intensity of the Q<sub>3</sub> signal decreases (Figure 4). These effects can be understood by considering that the presence of paramagnetic Cu<sup>2+</sup> ions provides an efficient relaxation pathway for the Si atoms that causes a general increase of the signal-to-noise ratio. This effect has been previously observed for Cu<sup>2+</sup> and other paramagnetic ions,<sup>61,62,64,65</sup> and actually, paramagnetic species are frequently used as additives to record <sup>29</sup>Si NMR spectra. For the Si atoms placed very close to the paramagnetic centers, the relaxation pathway provided by the Cu(II) centers is so effective that the NMR signals are so broadened that they disappear. Significant changes in the intensities of the <sup>29</sup>Si signals caused by paramagnetic species have been also previously observed.<sup>64,66</sup> The decrease of the Q<sub>3</sub> signal indicates that this effect is more important for Si atoms placed in Q<sub>3</sub> sites. It is evident that the Si atoms closer to the Cu<sup>2+</sup> ions are those corresponding to L' but these atoms are not observed in the NMR spectra because of the small amount of cryptand added. Thus, the NMR spectra indicate that L' is placed into the sol–gel network in Q<sub>3</sub>-rich sites, i.e., the need to accommodate the large cryptand causes a distortion of the surroundings that hinders the formation of four Si–O–Si connections. When Cu<sup>2+</sup> is coordinated to the N atoms of the cryptand, all the Si atoms in the surroundings are very efficiently relaxed and this causes a decrease of the  $I_{3/4}$  quotient.

Further evidence favoring the proposed interpretation comes from the spectra of the 5L'S and 25L'S samples after treatment with Cu<sup>2+</sup> (Table 1). The 5L'S sample was treated with a solution of Cu<sup>2+</sup> to form the Cu<sub>2</sub>L'-(OH)<sup>3+</sup> complex and then washed with water to release the excess of Cu<sup>2+</sup> ions trapped into the cavity network. The 25L'S sample was subjected to a similar treatment but following four previous reaction cycles with Cu<sup>2+</sup>, N<sup>3-</sup>, and H<sup>+</sup>. In both cases the presence of Cu<sup>2+</sup> causes a significant decrease of the  $I_{3/4}$  quotient with respect

**Table 2. Textural Data for Selected Samples Evaluated from the N<sub>2</sub> Adsorption–Desorption Isotherms<sup>a</sup>**

	sample			
	5L'S	50L'S	50L'/CuS	800LS
$S_{\text{BET}}$ (m <sup>2</sup> ·g <sup>-1</sup> )	137	445	323	172
$V_{\text{p}}$ (cm <sup>3</sup> ·g <sup>-1</sup> )	0.46	0.99	1.05	0.62
$D_{\text{th}}$ (nm)	6.2	5.5	8.7	7.4

<sup>a</sup> Porous volume ( $V_{\text{p}}$ ) and surface area ( $S_{\text{BET}}$ ) values were obtained using the BET method and the pore size ( $D_{\text{th}}$ ) was obtained by applying the Dollimore–Heal model.

to the Cu(II)-free samples. Moreover, the quotients in Table 1 reveal that the extent of the decrease depends on the concentration of L' in the xerogel, in agreement with the proposed interpretation. For the more diluted 5L'S sample, the  $I_{3/4}$  quotient decreases from 0.53 to 0.40 (24%), whereas for the more concentrated 25L'S and 50L'S samples the quotient decrease increases to 40% (25L'S) and 49% (50L'S).

The texture of the samples has been analyzed from the N<sub>2</sub> isotherms at 77 K of previously degassed xerogels. The samples selected for this study were 5L'S and 50L'S to check the effect of the cryptand content, and 50L'/CuS to detect possible changes associated with Cu(II) addition before gelation. A sample of the non-covalently bonded L cryptand (800LS) was also studied for comparative purposes. All these four cryptand–silica xerogels present N<sub>2</sub> adsorption–desorption isotherms with type IV shape and hysteresis loop typical of mesoporous materials.<sup>67</sup> From the isotherm analysis two main textural parameters are obtained: the specific pore volume  $V_{\text{pore}}$  (from the adsorption volume at saturation) and the specific surface area  $S_{\text{BET}}$  (by fitting to the BET equation in the lower relative pressure range).<sup>68</sup> The higher the cryptand concentration the higher the sample porosity and surface area but leading to a lower volume/surface ratio (Table 2), which suggests that the increase in the cryptand concentration does not induce larger pores in the network. Also noticeable is the effect in the porosity when the copper–cryptand complex is incorporated into the network. Thus, the 50L'/CuS sample shows the maximum pore volume, although at the same time there is an increase in the volume/surface ratio. Therefore, there is an additional pore size increase due to the copper complex. For the physically trapped L cryptand, 2 orders of magnitude larger concentrations in the starting solutions are required to observe texture effects similar to those found in the less concentrated sample of the L' cryptand.

From the analysis of the gas volume adsorbed at increasing relative pressures a distribution of the pore sizes in the sample can be inferred. This analysis is based on the Kelvin equation for the capillary condensation in the mesopores. It correlates the pore radius and the relative pressure when the capillary condensation takes place at each pore size. The method of Dollimore and Heal<sup>69</sup> calculates the pore size ( $D_{\text{DH}}$ ) using the Kelvin radius in a cylindrical pore model. This method has been applied to the adsorption branch of the isotherms and the positions of the distributions

(64) Peeters, M. J. P.; Wakelkamp, W. J. J.; Kentgens, A. P. M. *J. Non-Cryst. Solids* **1995**, *189*, 77.

(65) Méndez-Vivar, J.; Mendoza-Bandala, A. *J. Non-Cryst. Solids* **2000**, *261*, 127.

(66) Babonneau, F.; Maquet, J. *Polyhedron* **2000**, *19*, 315.

(67) IUPAC Rep. Physisorption Data for Gas/Solid System. *Pure Appl. Chem.* **1985**, *57*, 603.

(68) Brunauer, S.; Emmet, P. H.; Teller, E. *J. Am. Chem. Soc.* **1938**, *60*, 309.

(69) Dollimore, D.; Heal, G. R. *J. Appl. Chem.* **1964**, *14*, 109.

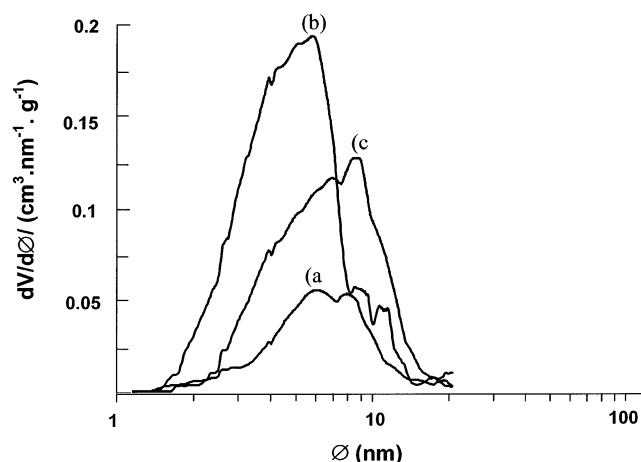


**Figure 5.** Pore size distribution for the 5L'S (a), 50L'S (b), and 50L'CuS (c) samples.

maxima are also shown in Table 2. Comparison of the pore size distribution plots (Figure 5) reveals that the distributions maxima remains at almost the same pore size when the L' content is increased but the whole distribution is shifted to lower pore sizes. Additionally, when the copper–cryptand complex is incorporated into the network the maximum goes to 8.7 nm with a wider pore size distribution. This behavior correlates with the fact that L' provides up to 18 sites for covalent binding with the xerogel network that can contribute to a better L'-silica matrix reticulation. Increasing the L' concentration induces a higher pore volume due to a larger number of pores rather than to an enlargement of pore size.

**Additional Studies on the Reactivity of the L'-Containing Xerogels.** The observation of a well-defined absorption band for the azide complex and the possibility of conducting a large number of reaction cycles without ligand leaching encouraged us to carry out additional studies to explore the possibility of using these materials for azide sensing. For this purpose, the samples 5L'S and 50L'S were selected, and the studies focused on both the quantitative response of the monoliths to the azide content in an external solution and on the response time of the monoliths to concentration changes. For the latter purpose, the kinetics of the reactions corresponding to complex formation and decomposition into the sol–gel matrix was studied.

The response of the monoliths to the azide concentration was evaluated by recording the absorption spectrum of the samples after treatment with the corresponding azide solution for 2 h. As expected, the intensity of the band at 375 nm increases with the azide concentration, with the response being linear up to concentrations close to  $1 \times 10^{-3}$  M (Figure 6). It is important to note that, although no special efforts had been made to optimize the response of these materials, a significant absorbance increase is observed for azide concentrations as low as  $5 \times 10^{-5}$  M, a value close to the detection limit of recently reported methods for the determination of azide.<sup>37–40</sup> Although the absorbance increase continues at higher concentrations of azide, the measured values deviate from the best-fit line shown in Figure 6. At very high azide concentrations it is expected that the sensing centers in the monolith become saturated, and actually, the measured absor-

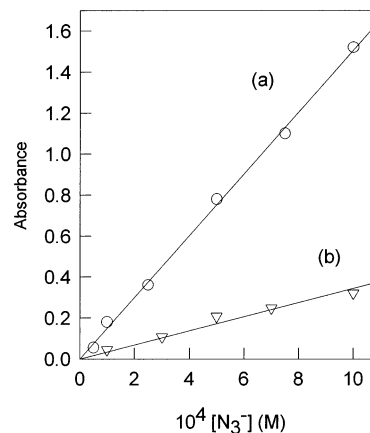


**Figure 6.** (a) Response of the 50L'S sample absorption at 375 nm to the azide concentration in an external solution. (b) Similar plot for a 5L'S sample stored at room temperature during 12 months.

bance is smaller than that predicted from extrapolation of the data at lower concentrations. An apparent value of  $K = (6 \pm 1) \times 10^2$  is obtained for the stability constant of the azide complex by fitting to eq 5<sup>70</sup> the absorbance data for all the azide concentrations.

$$Abs = \frac{aK[N_3^-]}{1 + K[N_3^-]} \quad (5)$$

The  $a$  parameter in eq 5, which includes contributions from the optical path length, the total concentration of  $Cu^{2+}$  complex, and the change in molar absorptivity upon formation of the azide complex, has a value of  $3.5 \pm 0.3$ . Although the value of  $K$  is smaller than that previously reported<sup>49</sup> in aqueous solution ( $6.6 \times 10^4$ ), the difference must be interpreted with caution because it includes not only the stability changes associated with trapping into the xerogels but also contributions from the different experimental conditions used in both studies.

As the development of sensors that work well under practical conditions also requires a rapid response to the external solution, we decided to obtain some information about the kinetics of the processes of complex formation and decomposition in the xerogels. We have previously shown<sup>49</sup> that the reactions in eqs 1–4 are rapid in aqueous solution for the nonsilylated L cryptand, with the equilibrium being attained in fractions of a second or a few seconds at concentrations similar to those used in this work. As the coordinating properties of L' are similar to those of L, only small differences in the kinetics of reactions are expected, and so, it can be reasonably assumed that reactions 1–4 are also rapid in aqueous solution for the case of L' (a kinetic study is not possible in this case because of the instability of L' in water solution). However, during the course of our previous work with xerogels containing trapped L,<sup>51</sup> we observed that the slow diffusion of the reagents through the cavity network of the xerogels made the reactions occur more slowly than in solution.

Some kinetic experiments of complex formation and decomposition in samples 5L'S and 50L'S were carried

(70) Connors, K. A. *Binding Constants. The Measurement of Molecular Complex Stability*; Wiley: New York, 1987; pp 139–168.

**Table 3. Kinetic Results for the Processes of Complex Formation and Decomposition at 25 °C in the 5L'S and 50L'S Samples**

sample	reagent	concentration (M)	$k_{\text{obs}}$ (s <sup>-1</sup> )	$k_{\text{obs}}$ (m <sup>3</sup> s <sup>-1</sup> )
5L'S	H <sup>+</sup> <sup>a</sup>	0.10	$(1.88 \pm 0.05) \times 10^{-3}$	$7.05 \times 10^{-10}$
5L'S	H <sup>+</sup>	1.0	$(1.32 \pm 0.01) \times 10^{-2}$	$4.95 \times 10^{-9}$
50L'S	H <sup>+</sup>	0.10	$(2.74 \pm 0.03) \times 10^{-3}$	$1.03 \times 10^{-9}$
50L'S	H <sup>+</sup>	1.0	$(2.14 \pm 0.01) \times 10^{-2}$	$8.02 \times 10^{-9}$
5L'S	Cu <sup>2+</sup> <sup>b</sup>	0.10	$(5.62 \pm 0.09) \times 10^{-4}$	$2.11 \times 10^{-10}$
50L'S	Cu <sup>2+</sup>	0.10	$(5.94 \pm 0.08) \times 10^{-4}$	$2.23 \times 10^{-10}$
5L'S	N <sub>3</sub> <sup>-</sup> <sup>c</sup>	0.0025	$(9.34 \pm 0.02) \times 10^{-4}$	$3.50 \times 10^{-10}$
5L'S	N <sub>3</sub> <sup>-</sup>	0.005	$(2.68 \pm 0.01) \times 10^{-4}$	$1.01 \times 10^{-10}$
5L'S	N <sub>3</sub> <sup>-</sup>	0.10	$(1.08 \pm 0.07) \times 10^{-4}$	$4.05 \times 10^{-11}$
50L'S	N <sub>3</sub> <sup>-</sup>	0.0025	$(1.06 \pm 0.02) \times 10^{-3}$	$3.98 \times 10^{-10}$
50L'S	N <sub>3</sub> <sup>-</sup>	0.005	$(2.95 \pm 0.03) \times 10^{-4}$	$1.11 \times 10^{-10}$
50L'S	N <sub>3</sub> <sup>-</sup>	0.10	$(1.10 \pm 0.09) \times 10^{-4}$	$4.12 \times 10^{-11}$
5L'S aged <sup>d</sup>	H <sup>+</sup> <sup>a</sup>	1.0	$(0.96 \pm 0.02) \times 10^{-2}$	$3.60 \times 10^{-9}$
5L'S aged	Cu <sup>2+</sup> <sup>b</sup>	0.10	$(3.07 \pm 0.08) \times 10^{-4}$	$1.15 \times 10^{-10}$
5L'S aged	N <sub>3</sub> <sup>-</sup> <sup>c</sup>	0.0025	$(1.06 \pm 0.02) \times 10^{-3}$	$3.98 \times 10^{-10}$

<sup>a</sup> Results corresponding to the decomposition of the Cu(II)-L-N<sub>3</sub><sup>-</sup> complex by treatment with a HNO<sub>3</sub> solution of the sample previously treated with Cu(II) and azide. <sup>b</sup> Results corresponding to formation of the Cu(II)-L complex by treatment of the sample with a Cu(NO<sub>3</sub>)<sub>2</sub> solution. <sup>c</sup> Results corresponding to the formation of the Cu(II)-L-N<sub>3</sub><sup>-</sup> complex by treatment with a NaN<sub>3</sub> solution of the sample previously treated with Cu(II). <sup>d</sup> Results obtained for a sample aged at room temperature for 12 months.

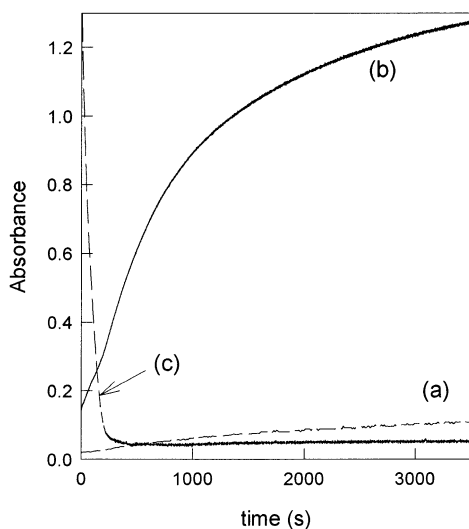


**Figure 7.** Selected kinetic traces for the reaction of the 5L'S sample with 0.1 M Cu<sup>2+</sup> (a), 0.0025 M N<sub>3</sub><sup>-</sup> (b), and 1.0 M H<sup>+</sup> (c). In all cases, the samples were washed with water during 1 h before starting the kinetic experiment.

out by treating the monolith with an external solution containing the desired reagent and recording the absorbance changes with time at wavelengths selected from the spectra shown in Figure 2. The experiments were carried out at 25 °C, and some typical examples of the kinetic curves obtained at 375 nm for the 5L'S sample are shown in Figure 7. The curves can be satisfactorily fitted by a single exponential to obtain the values of the pseudo-first-order rate constant ( $k_{\text{obs}}$ ), which is given in Table 3 both in s<sup>-1</sup> and m<sup>3</sup>s<sup>-1</sup>, the values in the latter units being obtained by considering the dimensions of the monolith and assuming the material to be homogeneous through the whole sample.

As expected, all the values of the rate constants (Table 3) indicate that the reactions are much slower in the sonogel pore network than in aqueous solution. In general, all the reactions are somewhat slower in the 5L'S sample than in 50L'S, although the differences between the two samples are usually smaller than those observed when the nature of the reagent in the external solution is changed. The observation of faster reactions for the 50L'S sample is consistent with the textural data

in Table 2: the pore size of both samples is significantly larger than the size of the reagents (H<sup>+</sup>, Cu<sup>2+</sup>, and N<sub>3</sub><sup>-</sup>) and allows their diffusion through the cavity network, but these diffusion processes are faster for the sample with a larger pore volume. The existence of significant differences in the values of the rate constant for the different reagents is surely reflecting the dependence of the diffusion rate on the nature of the reactants due to their different interactions with hydrogen-bonded silanol groups and water molecules in the xerogel.<sup>34,71,72</sup> As expected from the smaller size of the H<sup>+</sup> ion, complex decomposition in the presence of an excess of acid is always the fastest process, although the values of  $k_{\text{obs}}$  are still several orders of magnitude smaller than the corresponding values for reaction of the related Cu-L complex with H<sup>+</sup> in aqueous solution.<sup>49,51</sup> The effect of the concentration of N<sub>3</sub><sup>-</sup> on the rate of formation of the Cu-L-azide complex is unexpected because an increase in [N<sub>3</sub><sup>-</sup>] is accompanied by a decrease in the rate of complex formation. As the size of the azide ion (bite length of 2.34 Å) is significantly smaller than the pore size of the samples, the larger response times at higher concentrations seems to indicate a certain specific interaction of the N<sub>3</sub><sup>-</sup> anion with the silanol groups in the surface of the pores. The extent of such interaction is expected to increase with the azide concentration and lead to a reduced mobility of the anions and to a decrease in the rate of diffusion through the pore network.

These kinetic results indicate that the slow diffusion of the species constitutes a limitation to the potential use of these materials for sensing purposes. However, the large absorbance changes associated with the formation of the Cu-L'-azide complex allows the preparation of thinner monoliths in which the diffusion problems can be minimized while still maintaining a measurable response to the azide concentration. Actually, it is clearly observed that the color changes during the reaction cycles occur very rapidly at the external parts of the monoliths, and the reactions then progress

(71) Shamansky, L. M.; Yang, M.; Olteanu, M.; Chronister, M. *Mater. Lett.* **1996**, *26*, 113.

(72) Collinson, M. M.; Novak, B. *J. Sol-Gel Sci. Technol.* **2002**, *23*, 215.

more slowly toward the inner parts. The preparation of thin films from sols with a higher concentration of the cryptand is another alternative to solve the diffusion problems. Another problem for the potential sensing applications of these materials arises from the fact that regeneration of the monoliths after treatment with  $\text{Cu}^{2+}$  and  $\text{N}_3^-$  requires an excess of acid to achieve the complete decomposition of the complex, i.e., the simple treatment with water does not release the azide ions. However, once the diffusion problems are minimized, the need of an acid treatment should not represent a significant obstacle for the development of a rapid analytical procedure for azide determination.

As the properties of sol-gel materials may change with time, the long-term stability of the xerogels was also checked by studying the kinetics of the reactions with  $\text{Cu}^{2+}$ ,  $\text{N}_3^-$ , and  $\text{H}^+$  of a 5L'S sample that had been stored at room temperature for 12 months (all the previous reactivity studies were carried out 4 months after preparation of the samples). The values of the rate constants are included in Table 3 and differ only by a factor smaller than 2 from the corresponding previously determined values, which indicates that aging of the sample does not cause any significant change in the kinetics of reaction. In addition, the response of the aged sample to the azide concentration is also linear up to  $1.0 \times 10^3$  M (Figure 6b) and the quotient between the slopes of both plots in Figure 6 is 4.4, close to the quotient between the concentrations of L' in the starting sols (5.0). The binding constant for the formation of the azide complex with the aged 5L'S sample is  $(5.5 \pm 0.07) \times 10^2$ , which agrees within errors with the value derived for the 50L'S sample. These results clearly show that aging of the samples must not represent any important problem for the potential sensing applications of these materials. Moreover, the whole set of results in the present paper indicate that a coordination chemistry quite similar to that observed in aqueous solution can be developed for these binuclear cryptates, which can be exploited for the design of new materials in which the ability of this kind of cryptand for the selective recognition of species in solution is maintained.

### Experimental Section

**Reagents.** Copper sulfate, carbonate, tris(2-aminoethyl)-amine, isophthalaldehyde, and 3-chloropropyltriethoxysilane were obtained from Aldrich. TEOS was purchased from Merck, and formamide, EtOH, and phosphate buffer were from Panreac. Acetonitrile, pentane, methanol, and  $\text{CD}_3\text{CN}$  were obtained from SDS. The cryptand L was obtained as L.6HBr using the literature procedure.<sup>48</sup> Standard Schlenck and syringe techniques were used for the synthesis and handling of L'.

**Synthesis of L'.** A mixture of 1.33 g (1 mmol) of L.6HBr, 1.27 g (12 mmol) of  $\text{Na}_2\text{CO}_3$ , and 1.52 g (6 mmol) of  $\text{Cl}(\text{CH}_2)_3\text{-Si}(\text{OEt})_3$  in 150 mL of acetonitrile was refluxed for 20 h under an argon atmosphere. After elimination of the acetonitrile solvent under reduced pressure, the inorganic salts were precipitated by addition of 100 mL of pentane. The solid was separated by filtration and pentane was evaporated under reduced pressure, which led to isolation of L' as an oily liquid (0.87 g, 47% yield). NMR spectra in  $\text{CD}_3\text{CN}$ :  $\delta_{\text{H}}$  7.15–7.25 (m, 12H, aromatic), 3.82 (q, 36H,  $\text{CH}_2\text{-CH}_3$ ), 3.60 (s, 12H, N- $\text{CH}_2\text{-C}_{\text{aromat}}$ ), 3.59 (t, 12H, N- $\text{CH}_2\text{-CH}_2\text{-CH}_2\text{-Si}$ ), 2.61 and 2.68 (dt, 24H, N- $\text{CH}_2\text{-CH}_2\text{-N}$ ), 1.84 (m, 12H, N- $\text{CH}_2\text{-CH}_2\text{-CH}_2\text{-Si}$ ), 1.20 (t, 54H,  $\text{CH}_2\text{-CH}_3$ ), and 0.72 (m, 12H, N- $\text{CH}_2\text{-CH}_2\text{-CH}_2\text{-Si}$ );  $\delta_{\text{C}}$  128.2, 129.0, 129.2, and 140.7 (aromatic), 59.1 ( $\text{CH}_2\text{-CH}_3$ ), 53.6 and 54.9 (N- $\text{CH}_2\text{-CH}_2\text{-N}$ ), 48.4 and 48.5 (N- $\text{CH}_2\text{-C}_{\text{aromat}}$  and N- $\text{CH}_2\text{-CH}_2\text{-CH}_2\text{-Si}$ ), 27.4 (N- $\text{CH}_2\text{-CH}_2\text{-CH}_2\text{-Si}$ ), 18.6 ( $\text{CH}_2\text{-CH}_3$ ), and 8.5 (N- $\text{CH}_2\text{-CH}_2\text{-CH}_2\text{-Si}$ );  $\delta_{\text{Si}}$  -43.3.

### Preparation of the L'-Containing Sol-Gel Materials.

An L' solution was prepared from 0.123 g of the aforementioned oily liquid diluted in 50 mL of a 50% mixture of EtOH-acetonitrile and kept in a dry atmosphere. Taking into consideration the different hydrolysis rates of both alkoxides, ultrasound-assisted prehydrolysis of TEOS was performed as described elsewhere.<sup>51</sup> The L'S samples were prepared by addition of different amounts of L' solution to the resulting silica sonosol. Formamide was added as a drying control chemical additive (DCCA) in a  $R_f = 4$  TEOS/formamide molar ratio. The same procedure was followed for the preparation of CuL'S samples but by using a  $\text{CuSO}_4$  saturated acidic water solution in the prehydrolysis step. For comparison purposes, a xerogel containing physically trapped ligand, L, was prepared by the route described in a previous paper.<sup>51</sup> In all cases, the doped sol was transferred to sealed PVC cuvettes and left to gel at room temperature. Gelation time varied from 4 to 1 days depending on the L' content. After an aging period of one week and drying for another week in an oven at 40 °C in unsealed containers, monolithic pieces (15 × 5 × 5 mm) of stable samples resulted.

**Instrumentation.** The UV-Vis spectra were recorded with a Varian CARY 1 3E spectrophotometer. The NMR spectra, both in solution and in the solid state, were recorded with a Varian Unity 400 spectrometer, and the chemical shifts in the  $^1\text{H}$ ,  $^{13}\text{C}$ , and  $^{29}\text{Si}$  spectra were reported in ppm with respect to tetramethylsilane (TMS). The solid state  $^{29}\text{Si}$  MAS spectra were recorded at 5 kHz using short pulses (5  $\mu\text{s}$ ) and a long delay between pulses (20 s); the total number of transients acquired was 512 in all cases. The porosity studies were carried out by making nitrogen physisorption experiments at 77 K with a Sorptomatic 1900 Fison instrument.

**Acknowledgment.** Financial support by the Spanish Ministerio de Ciencia y Tecnología (Research Projects BQ2000-0232 and MAT2000-0468-P4-02) is gratefully acknowledged. We also acknowledge J. M. Duarte (Servicios Centralizados de Ciencia y Tecnología, Universidad de Cádiz) for his assistance with the solid state NMR experiments.

CM021337Y